

# Spatial variability of marine heatwaves in the Chesapeake Bay

## Authors:

Rachel Wegener	University of Maryland, College Park	rwegener@umd.edu
Jacob Wenegrat	University of Maryland, College Park	wenegrat@umd.edu
Veronica Lance	National Oceanic and Atmospheric Administration (NOAA) National Office of Satellite Data and Information Service, Center for Satellite Applications and Research, and NOAA Coastwatch	veronica.lance@noaa.gov
Skylar Lama	School of Earth and Atmospheric Science and the Program of Ocean Science and Engineering, Georgia Institute of Technology	slama8@gatech.edu

**Peer review status:** This is a non-peer-reviewed preprint submitted to EarthArXiv.

This manuscript is in review at the journal Estuaries and Coasts (ESCO). Subsequent versions of this manuscript may have different content. If accepted, the final version of this manuscript will be available via the 'Peer-reviewed Publication DOI' link via this webpage.

# Spatial variability of marine heatwaves in the Chesapeake Bay

Rachel Wegener<sup>1\*</sup>, Jacob Wenegrat<sup>1</sup>, Veronica P. Lance<sup>2</sup>,  
Skylar Lama<sup>3, 4</sup>

<sup>1\*</sup>Department of Atmospheric and Oceanic Science, University of Maryland, College Park, 4254 Stadium Drive, College Park, 20742, MD, USA.

<sup>2</sup>National Oceanic and Atmospheric Administration (NOAA) National Office of Satellite Data and Information Service, Center for Satellite Applications and Research, and NOAA Coastwatch, 5830 University Research Court, College Park, 20740, MD, USA.

<sup>3</sup>School of Earth and Atmospheric Science, Georgia Institute of Technology, 311 Ferst Dr, Atlanta, 30332, GA, USA.

<sup>4</sup>Ocean Science and Engineering, Georgia Institute of Technology, 311 Ferst Dr, City, 30332, Atlanta, GA.

\*Corresponding author(s). E-mail(s): [rwegener@umd.edu](mailto:rwegener@umd.edu);  
Contributing authors: [wenegrat@umd.edu](mailto:wenegrat@umd.edu); [veronica.lance@noaa.gov](mailto:veronica.lance@noaa.gov);  
[slama8@gatech.edu](mailto:slama8@gatech.edu) ;

## Abstract

The Chesapeake Bay is the largest and one of the most productive estuaries in the United States. Like many estuaries, rising global temperatures have impacted this ecologically important zone. Marine heatwaves, extreme temperature events, are increasingly common in the Chesapeake Bay. Although marine heatwaves evolve across space and time, a complete spatial picture of marine heatwaves in the Bay is missing. Here we use satellite sea surface temperature data to characterize marine heatwaves in the Chesapeake Bay. We consider two products: NASA MUR and NOAA Geo-Polar, and validate their effectiveness for studying marine heatwaves in an estuary using in situ data from the Chesapeake Bay Program. A north-south (along estuary) gradient is identified as a common pattern of spatial variability, seen in both marine heatwave duration and number of events. Our satellite-based approach enables us to analyze marine heatwaves in Chesapeake Bay tributaries for the first time, and finds marine heatwaves in

these regions to display different characteristics from the main stem of the Bay. For example, marine heatwave maximum intensity is higher in tributary waters. Long term trends in marine heatwave characteristics are also analyzed, although confidence in long term trends is tempered by changes in satellite error over time, pointing to the criticality of periodic reanalyses of satellite data to identify and correct for systematic error. MHW analysis with a detrended baseline suggests the major observed spatial patterns are a result of long term warming not a shifting temperature distribution. The differing spatial patterns suggest that there are different physical influences in the main stem of the Bay and in the tributaries. This work affirms that satellite data can be an effective tool for studying marine heatwaves in estuaries and enables similar studies in other estuaries.

**Keywords:** marine heatwaves, sea surface temperature, estuary, Chesapeake Bay, satellite remote sensing

## 1 Introduction

Anthropogenic climate change is raising global temperatures, both through an increasing global average temperature and through an increasing number of extreme temperature events (Rahmstorf and Coumou, 2011). One of these increasingly common extreme events is Marine Heatwaves (MHWs), prolonged periods of anomalously warm water (Oliver et al, 2019). Extreme temperature changes such as MHWs affect marine ecosystems on the individual, population, and community levels (Smith et al, 2023). Not all MHWs are the same, however, and the ecosystem response depends on the characteristics of the MHW, such as the duration and rate of onset (Smith et al, 2023). These ecosystem impacts translate into socioeconomic impacts. In the US alone economic losses through October 2022 "of single MHW events exceed US\$800 million in direct losses and in excess of US\$3.1 billion per annum in indirect losses for multiple consecutive years" (Smith et al, 2021). MHWs and their ecological and economic impact are unfortunately part of our warming world.

The Chesapeake Bay is the largest and one of the most productive estuaries in the United States (Bilkovic et al, 2019). The Chesapeake Bay has seen a trend of long term warming (Hinson et al, 2022) and increasing temperatures have been linked to growing hypoxic conditions in the Bay (Du et al, 2018). In addition to long term warming, previous work has identified MHWs in the Chesapeake Bay using buoy data (Mazzini and Pianca, 2022; Shunk et al, 2024). Extreme temperatures in 2005 caused an over 50% loss in the seagrass species *Z. marina* in which fisheries species find nursery habitat (Lefcheck et al, 2017). As a result, the area saw declines in three commercially important fish species (Smith et al, 2023). A recent report by the Scientific and Technical Advisory Committee, an independent group which provides scientific and technical guidance on environmental issues in the Chesapeake Bay, specifically highlighted the need to develop a marine heatwave warning system due to the impact on living resources (Batiuk et al, 2023).

Here we use sea surface temperature (SST) satellite data to evaluate the occurrence and characteristics of MHWs in the Chesapeake Bay over a 20 year period, looking at

average characteristics as well as long term trends. We specifically focus on patterns in the characteristics of MHW, critical for assessing the potential ecological impact, and as potential guidance towards understanding mechanisms. We do this at a new level of geographic detail, as satellite data enables spatial coverage that is not possible with in situ data alone. Past work using buoys did not find significant differences between the surface expressions of MHW characteristics in the different regions of the Chesapeake Bay (Mazzini and Pianca, 2022), however we find that there is spatial variation in the surface expression of several defining characteristics of MHWs. Finally, the use of satellite data to investigate MHWs in an estuary setting is novel. Despite the relatively limited horizontal resolution of the observations relative to the size of the Bay, the results and validation presented here suggest this approach can be useful for understanding both temporal and spatial variability of MHWs in estuarine ecosystems such as the Chesapeake Bay.

In section 2 we introduce the chosen datasets and describe the definition of MHWs and MHW characteristics. In section 3 we discuss the validation of the satellite data. We also discuss the spatial and temporal patterns in MHWs characteristics. In section 4 we conclude by summarizing our major findings and propose routes for future analysis.

## 2 Methods

### 2.1 Satellite Data Sources

The satellite data products potentially suitable for this study are those with a fine spatial grid and a long operating period. The need for high spatial grid is driven by the size of the Chesapeake Bay. The need for a long operating period is driven by the baseline climatology required for MHW calculations. Hobday et al (2016) recommends a 30 year climatology. However, past work has shown no appreciable difference in MHW duration or intensity calculated from climatologies based on records as short as 10 years when compared with those calculated using the recommended 30 year time series (Schlegel et al, 2019).

Two satellite SST products fulfilling these criteria were evaluated as candidates for this study: NASA MUR v4.1 and NOAA Geo-Polar Blended v2.0. NASA MUR is a daily  $\sim 1\text{km}$  level 4 product based on nighttime SST observations and provides an estimate of the foundation temperature (Chin et al, 2017). Foundation temperature, as defined by the Group for High Resolution Sea Surface Temperature (GHRSSST), is the temperature at a depth free of diurnal variability (Beggs, 2020). NOAA Geo-Polar is also a daily level 4 product, and has  $\sim 5\text{km}$  grid resolution (Maturi et al, 2017). Geo-Polar nighttime SST is used in order to decrease the influence of diurnal variation in the surface temperatures, thereby maintaining a SST definition that is comparable between Geo-Polar and MUR. See Table 1 for a summary of the two datasets. Both datasets are gap filled for clouds. Seven days of data in the Geo-Polar dataset were removed by NOAA data processing due to quality control. These missing 7 days were linearly interpolated in time for each pixel when generating the climatology.

**Table 1** Satellite SST Data Sources

Product Name	Version	Organization	Spatial Grid	Temporal Resolution	Availability
MUR	4.1	NASA	$0.01^\circ$ ( $\sim 1\text{km}$ )	daily	May 31, 2002 - present
Geo-Polar Blended	2.0	NOAA	$0.05^\circ$ ( $\sim 5\text{km}$ )	daily	Sept. 1, 2002 - present

## 2.2 Marine Heatwave Calculation and Characteristics

[Hobday et al \(2016\)](#) established the canonical definition of a MHW: a MHW occurs when the temperature rises above the 90th percentile temperature for that day and persists above the daily 90th percentile value for at least 5 days. This is illustrated in Figure 1 panel A. If an event exceeds the 90th percentile threshold but does not last 5 days it is called a heat spike. The time period for the climatology is the full dataset time period, Jan. 1, 2003 to Dec. 31, 2022 (20 years). Again following [Hobday et al \(2016\)](#), the 90th percentile threshold for each day uses the days from a centered 11 day window. After the threshold is calculated, the values are smoothed using a 31 day moving average. If multiple MHW longer than 5 days occur within two days of each other they are considered to be a single MHW event. MHWs were calculated using the Python software package `marineHeatWaves` ([Oliver, 2023](#)). The procedures described above are the defaults of this package, and are consistent with the recommendations in [Hobday et al \(2016\)](#).

While most of the analysis presented here used the MHW definition from [Hobday et al \(2016\)](#), we also performed our analysis using a linearly detrended SST. To do this we performed a linear fit on the satellite SST timeseries, then subtracted the trend from the SST. After removing the long term trend the remained of the MHW calculation was calculated as described in the previous paragraph. These results are discussed in section 3.3 below.

MHW characteristics allow us to consider different types of MHW. Two extreme temperature events could both be MHW, but still have very different characteristics and thus correspond to different ecological impacts or physical processes of development. The 6 characteristics analyzed in this study are: 1) number of annual events, 2) duration, 3) maximum intensity, 4) cumulative intensity, 5) rate of onset, and 6) rate of decline. Figure 1 panel B shows a graphic representation of the MHW characteristics for an example heatwave in July 2020 (see also ([Hobday et al, 2016](#))).

## 2.3 Satellite Data Validation

In situ data compiled by the Chesapeake Bay Program (CBP) was used to validate satellite SST in the Chesapeake Bay. The database contains measurements from the CBP partner organizations at long-term, fixed monitoring stations. *Traditional Partner Data* from all the programs was used.

The satellite datasets both estimate foundation SST. The in situ data, on the other hand, provide measurements of SST at multiple times of day and depths. To

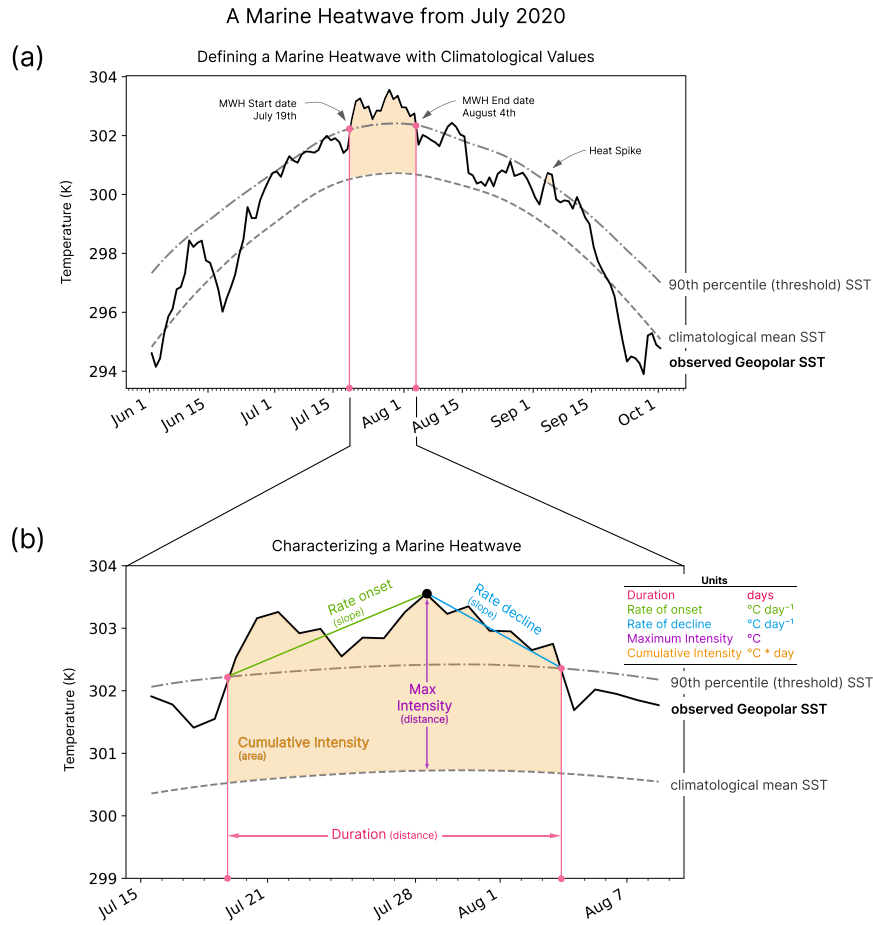


**Fig. 1** The observed and climatological values of a MHW from July 2020 in the Tangier Sound in the Middle Chesapeake Bay ( $38.03^{\circ}\text{N}$ ,  $75.97^{\circ}\text{W}$ ), illustrating the definitions of a MHW and MHW characteristics defined in [Hobday et al \(2016\)](#). Panel (a) visualizes a sustained temperature anomaly exceeding the 90th percentile threshold value defining a MHW. Panel (b) shows SST focused on the heatwave period, labeling the 5 MHW statistics used in this study to characterize MHWs.

approximate the foundation temperature values from the in situ dataset, only temperature values between 1 and 3 meters depth were used. This was done to avoid very near-surface measurements, which are likely subject to stronger diurnal temperature fluctuations. The sensitivity of this depth choice was tested by computing the RMSE between in situ and satellite SST values with several depth choices ranging from 0.5-7m. The RMSE changed by  $0.1^{\circ}\text{C}$  or less in all depth choices. The validation period was a 20 year period from Jan. 1, 2003 to Dec. 31, 2022.

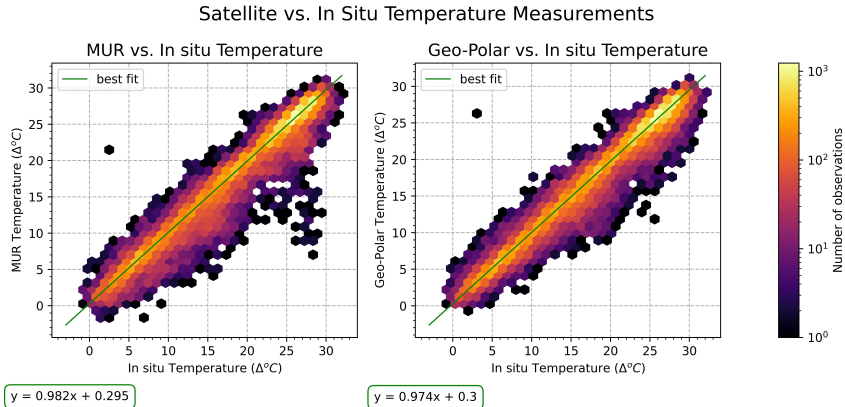


**Fig. 2** Density plots of the temperature error for MUR SST and Geo-Polar SST, as compared to the Chesapeake Bay Program (CBP) in situ dataset. The left panel shows MUR and the right panel shows Geo-Polar. Green lines on each plot show the linear fit of observations. Geo-Polar has a tighter fit than MUR, while both datasets underestimate extreme values.

To evaluate the accuracy of the two satellite datasets, the observed temperature from each satellite dataset was compared to in situ observations. Both satellites have RMSEs of less than  $2^{\circ}C$ , with Geo-Polar performing slightly better (Table 2). MUR had more outliers (Figure 2). Both datasets are most accurate in the main stem of the Bay and least accurate closer to shore (Figure 3). Geo-Polar has the largest errors in the upper Potomac and the outflow of the Susquehanna River, while MUR has the largest errors on the western shore rivers north of Baltimore, such as the Gunpowder and Bush Rivers. MUR also generally has higher mean error than Geo-Polar near the Eastern shore.

**Table 2** Satellite SST Mean Errors

Product Name	Slope	Intercept ( $^{\circ}C$ )	RMSE ( $^{\circ}C$ )
MUR	0.98	0.30	1.81
Geo-Polar Blended	0.97	0.30	1.56

As extreme temperature events, MHWs are deviations from a climatological mean. Because of this, error in the climatological SST value do not affect the MHW calculation. Here we evaluate the accuracy of the satellite SST measurements for use in calculating MHWs using the error in the anomaly from climatology as opposed to the error in the raw SST value. This method of validation better reflects expected errors in our MHW analysis.

To compare the satellite and in situ data, a 20 year climatology was computed for satellite and in situ datasets. Of the several hundred stations in the CBP dataset, 49 stations were identified with sufficient temporal coverage to compute a climatological baseline. There is a consistent seasonal sampling bias among the CBP in situ stations, in which summers are more highly sampled than winters (Figure 4). To minimize the

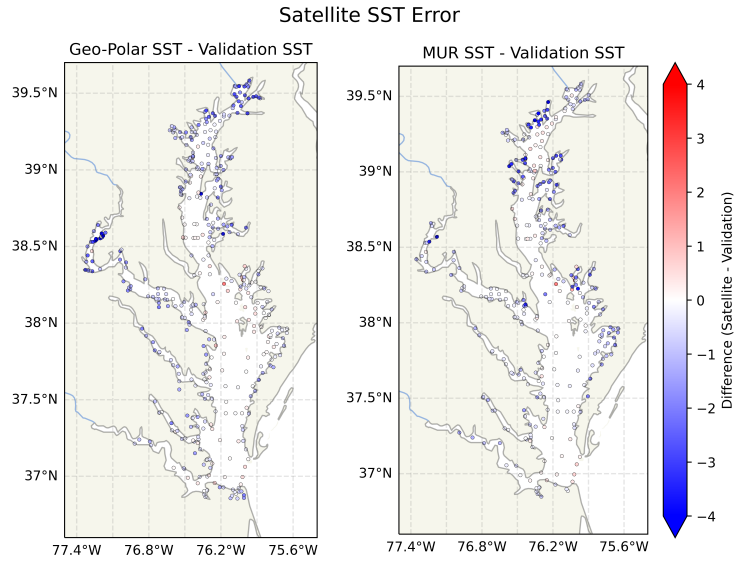


**Fig. 3** Spatial distribution of the mean error between the satellite SST datasets and the Chesapeake Bay Program in situ data. Both datasets are most accurate in the main stem of the Bay and have the largest errors near shore. The areas of largest error vary between the two satellites.

impact of this bias on our analysis, stations were vetted by both number of observations and monthly consistency of observations. A station needed to have at least one observation every month in at least 60% of the years. It was also required to have at least one observation per month in 10 of the 12 months in 90% of the years.

Figure 4 shows the spatial distribution of the validation stations. The most important area for our analysis, the main stem of the Bay, is well covered by validation stations, with the exception of one portion of the lower bay. The Potomac River and Susquehanna outflow are also well covered, as are many of the Eastern shore river outflow regions in the upper and middle bay. The major lower bay rivers, however, including the Rappahannock, the York, and the James, do not have any useable validation stations. We therefore focus our analysis of tributaries primarily on those with validation stations. Validation data is important for assessing the effectiveness of space-borne satellite monitoring for estuaries such as the Chesapeake Bay. Increased in situ observations in the under-sampled areas of the Bay would be valuable to future investigations.

Finally, we evaluated the likelihood that errors in satellite measurements would correlate temporally causing spurious MHWs. To do this we computed the temporal autocorrelation of the error in water temperature anomaly from climatology. The in situ dataset does not provide the temporal resolution to compute autocorrelation with a daily lag, so buoy data from NOAA's Chesapeake Bay Interpretive Buoy System (CBIBS) was used instead. We selected 3 buoys, one each in the Upper, Middle, and Lower Bay (Figure 3). The Upper Bay buoy only had about 6 years of observations, but was still included for spatial coverage. Only nighttime (12am-7am local time) buoy measurements were used to match the satellite SST foundation temperature definition



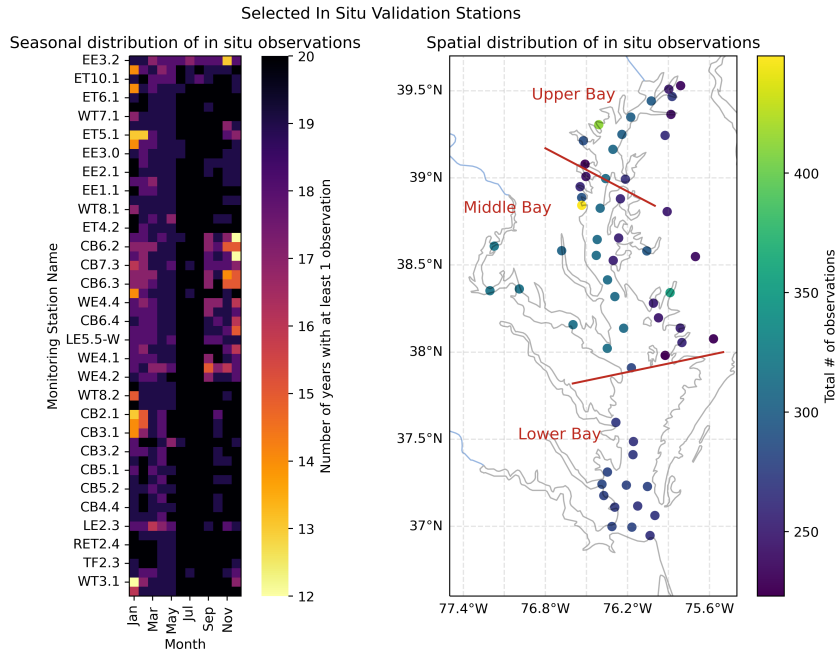


**Fig. 4** The left panel shows the monthly distribution of in situ observations for each of the validation stations used. Color shows the number of months in the 20 year time series that had at least one observation. The right plot shows the spatial distribution of validation stations, colored by the total number of observations. Validation stations cover the majority of the main stem of the Bay and several important tributaries. There is a seasonal bias in observations, however winter months are still represented.

and missing data in the buoy record was dropped when calculating autocorrelation. The decorrelation timescale was computed and defined as the number of days at which the autocorrelation dropped below  $e^{-1}$ .

**Table 3** CBIBS Buoy Data Sources

Buoy Name	Section	Approx. Latitude	Approx. Longitude	Operating Years	No. of Days of Observations
Annapolis	Upper	38.96°N	76.45°W	2013-present	2308
Goose's Reef	Middle	38.56°N	76.42°W	2011-present	3107
Stingray Point	Lower	37.57°N	76.26°W	2012-present	3532

## 2.4 Effects of Satellite SST Errors on Marine Heatwave Calculations

Using satellite SST in the narrow Chesapeake Bay pushes the limits of these satellite datasets. To understand the potential impact of satellite data on the robustness of the

**Table 4** Satellite SST Anomaly Mean Errors

Product Name	Slope	Intercept ( $^{\circ}\text{C}$ )	RMSE ( $^{\circ}\text{C}$ )
MUR	0.64	0.04	1.75
Geo-Polar Blended	0.59	-0.10	1.38

MHW analysis, we considered the following forms of error: 1) mean error 2) frequency distribution (histogram) of satellite errors 3) temporal autocorrelation of error 4) long term and seasonal variability in satellite errors 5) spatial variability in satellite errors. Not all forms of errors in the satellite SST product, however, will propagate to the MHW calculation in the same way.

To assess the mean error between the satellite and in situ SST anomaly estimates slope and root mean squared error (RMSE) were used (Table 4). Due to the presence of outliers in this dataset regressions were computed using a robust linear regression with a Tukey Biweight norm. Results from the two satellite datasets were quantitatively similar, with Geo-Polar performing slightly better in RMSE. The slopes of less than 1 with intercepts close to 0 indicate that both datasets underestimate extreme values, suggesting that our results could be an underestimate of extreme events. These relationships can also be seen in the distributions of Figure 5. Underestimates in extreme values would result in lower maximum intensities and could also contribute to lower cumulative intensity, rate of onset, and rate of decline. Due to the lower RMSE we chose to calculate MHW using the Geo-Polar Blended SST product. The remainder of our validation results are therefore only shown for Geopolar.

For the purposes of MHWs, errors need to be adjacent in time to produce false MHW. To evaluate this we estimate the error decorrelation timescale. For all 3 of the tested buoys the decorrelation timescale was either 3 or 4 days, less than the 5 day minimum length of a MHW. So while the SST mean errors are non negligible they decorrelate on a timescale shorter than the threshold for MHW identification.

Temporal variation is another important form of potential bias in satellite errors. A Hovmöller plot shows there is not consistent seasonality in anomaly errors (Figure 6). Summers, however, do show a long term trend in error from March through August. These months underestimate anomaly values prior to 2011 and overestimate anomaly values in 2011 onward. This increasing long term error could lead to an overestimate in the long term trend in summertime MHW occurrences and intensity, discussed further in section 3.3.

Spatially, the mean error displayed very little variation (Figure 7), indicating that spatial variations in MHW, the focus of this paper, are likely not unduly influenced by satellite errors. In contrast, the long term trend in the error was largest in the upper bay and insignificant in most of the lower bay. Several of the lower bay tributaries, including the Rappahannock, the York, and the James Rivers, did not have any validation stations (Figure 4). Because of this we proceed with caution when interpreting results in these tributaries.

We note the primary caveat in our validation analysis is uncertainty in the approximation of foundation temperature from the in situ data for comparison with satellite

### Satellite vs. In Situ Anomaly Measurements

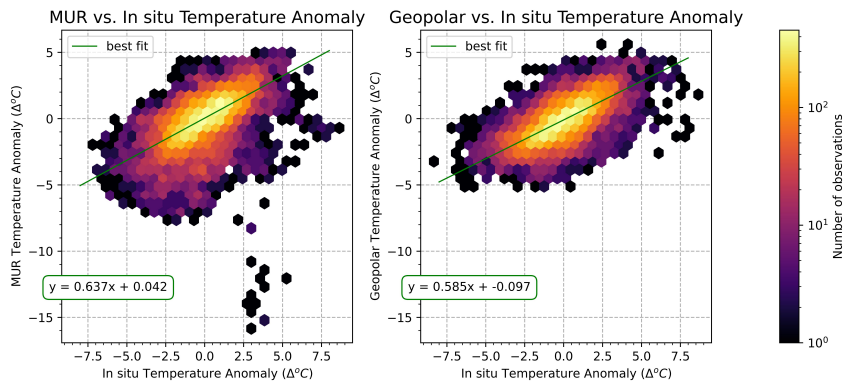


**Fig. 5** Density plots of the anomaly error for MUR SST and Geo-Polar SST, as compared to the Chesapeake Bay Program (CBP) in situ dataset. The left panel shows MUR and the right panel shows Geo-Polar. Green lines on each plot show the linear fit of observations. Geo-Polar has a tighter fit than MUR, while both datasets underestimate extreme values.

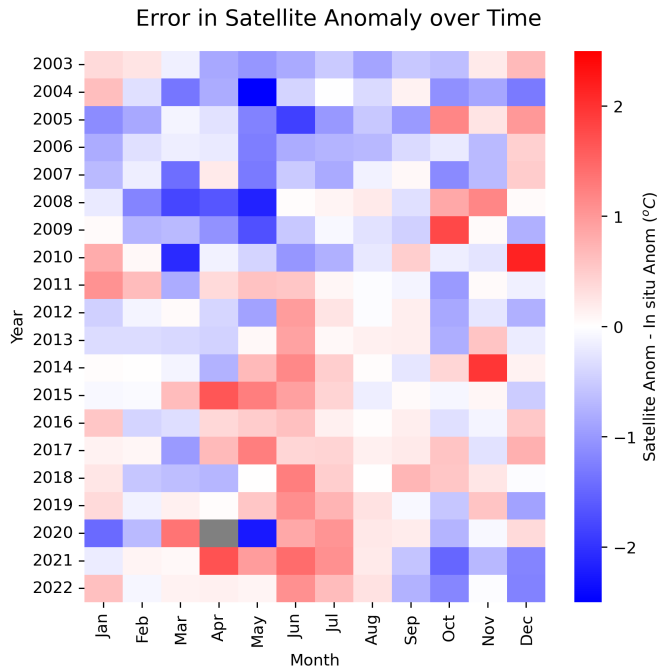


**Fig. 6** The error in SST anomalies from climatology for Geo-Polar by month and year. Each pixel corresponds to the average satellite error for all pixels in the Bay during that year (x axis) and month (y axis). The colorbar shows satellite SST minus in situ measurements, such that negative (blue) values represent satellite SST underestimates of in situ temperature. Geo-Polar SST has a long term trend in the error in SST anomaly from climatology over time in summer months, but no consistent seasonal error.

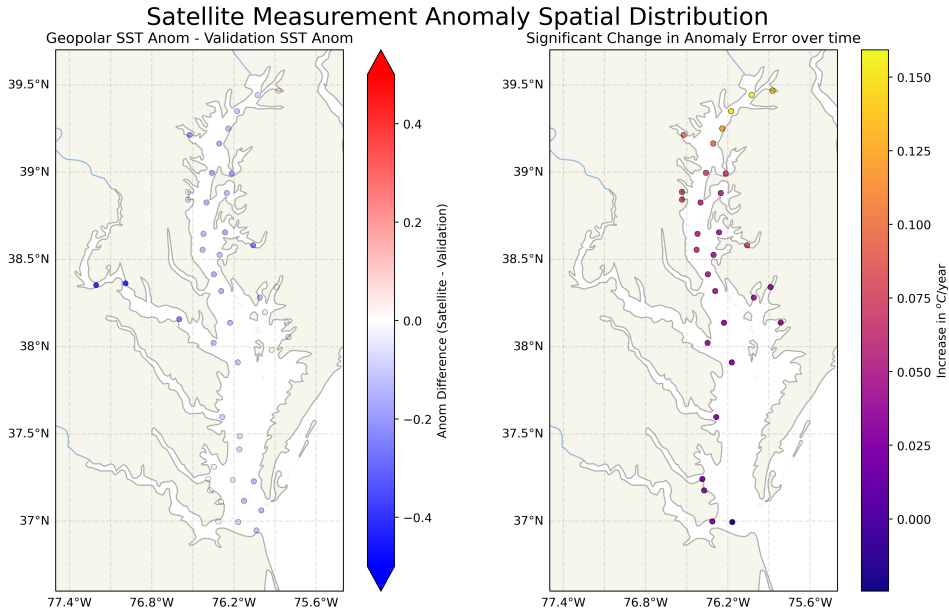


**Fig. 7** Maps display the spatial distribution of error across the validation stations. The left figure shows the mean error. The right figure shows the long term trend in the error. Only stations with a significant trend are displayed ( $p$  value less than 0.05). Mean error is consistent throughout the Bay, but long term trend in error shows a north/south gradient, discussed further in section 3.3.

SST. This error, however, is difficult to assess fully without in situ observations at additional depths to more robustly determine the foundation depth. Overall, we expect our analysis underestimates the maximum intensity, and may overestimate the strength of long term trends. However, the fast decorrelation timescale of errors relative to the MHW identification threshold is expected to limit the effect of errors on the identified patterns of MHW characteristics. We address the relative magnitudes of these effects in the context of our results in the next section (3).

## 3 Results

### 3.1 Temporal Marine Heatwave Characteristics

Many major documented MHW in the Northwest Atlantic Ocean also appear in the Chesapeake Bay, including MHWs in summer 2012 (Mills et al, 2013), winter 2015-2016/fall 2016 (Pershing et al, 2018), and early spring 2017 (Gawarkiewicz et al, 2019). One MHW of particular interest for the Bay was a September 2005 heatwave, during which anomalously high temperatures were shown to decrease commercially relevant seagrass habitat (Smith et al, 2023). The evolution of this MHW is shown in Figure 8 as an example of the capabilities of the satellite data and to contextualize the aggregate statistics presented later. The MHW first emerged in the center of the Bay, expanded to encompass most of the main stem by the peak, then receded beginning in the upper Bay. The last area to experience high temperatures was the mouth of the

Evolution of a September 2005 MHW

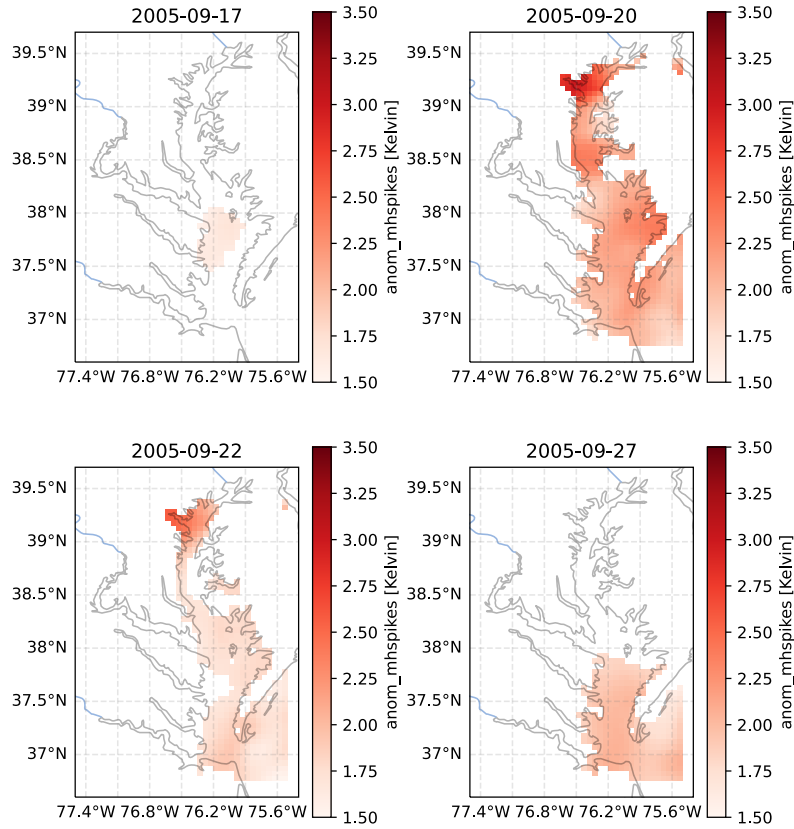


**Fig. 8** Evolution of temperature anomaly during a 2005 MHW. The 4 panels show 4 dates throughout the MHW: September 17th, September 20th, September 22nd, and September 27th. Only pixels with an identified MHW are plotted.

Bay. The strongest anomalies were in the upper bay near Baltimore. While this MHW affected the full Bay and decayed toward the Bay mouth, other MHW show different patterns of spatial evolution. For example, some MHW begin in the river outflow regions. Additional work could consider these different spatial patterns of evolution and decline, as they may give insight into different driving mechanisms.

The frequency of MHW in the Chesapeake Bay is increasing over time (Mazzini and Pianca, 2022), consistent with the global trend (Oliver et al, 2018). Figure 9 shows the number of annual MHW events over time in the upper, middle, and lower sections of the Bay. All SST pixels over each of the three sections were averaged together to generate a single annual result. The results from our analysis are shown alongside results from Mazzini and Pianca (2022), which derive MHW frequency from buoy data. There is good agreement between the buoy-derived MHW frequency and the satellite-derived MHW frequency. Mazzini and Pianca (2022) found that there were on average 2 MHW per year with an average duration of 11 days per year, resulting in

Long term trend in MHW frequency: Buoy and satellite datasets

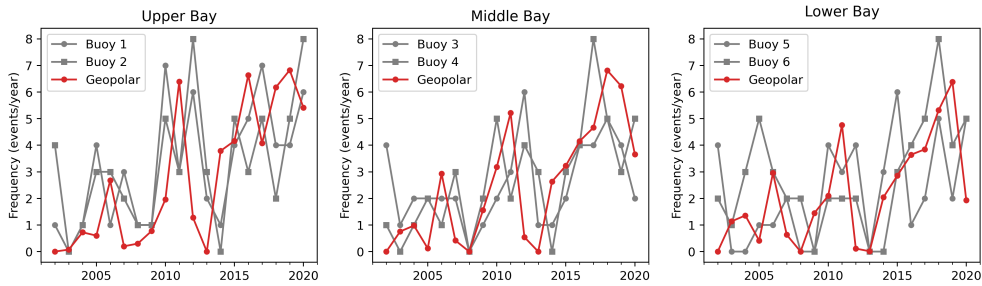


**Fig. 9** Time series of MHW frequency in the upper, middle, and lower sections of the Chesapeake Bay. (See Figure 4 for Bay regions). Frequency of MHW is increasing in all three regions of the Bay. Frequency calculated using Geo-Polar SST, plotted in red, is shown alongside MHW frequency derived from buoys, plotted in gray. Buoy-derived MHW frequency was reported in [Mazzini and Pianca \(2022\)](#). Regional MHW frequencies are consistent between Geo-Polar and buoy-derived MHW characteristics.

an average of 22 MHW days per year. The satellite derived MHW produce consistent results, with a bay-wide average of 2.3 events per year and 10.8 days / event for a total of 25 MHW per year. Comparison of these results with [Mazzini and Pianca \(2022\)](#) provides a further form of validation of our approach.

Because MHW are defined relative to a daily climatological baseline, MHW can occur at any time of the year. Figure 10 shows monthly aggregations of MHW for the 6 MHW characteristics. Each MHW in the dataset is counted once and grouped into the month in which it started. In the Chesapeake Bay, MHWs are most prevalent in the Summer with a secondary spike in January. [Mazzini and Pianca \(2022\)](#) also found a summertime peak in MHW, however because [Mazzini and Pianca \(2022\)](#) aggregate by season instead of month it is not clear if their buoy-based analysis also showed a January spike. MHW duration has an inverse relationship to the number of MHWs, with duration peaks in March and December. Maximum and cumulative intensity follow the duration pattern, indicating that MHW that begin in March or December are the longest lasting and have high maximum intensities. A subsurface MHW study by [Shunk et al, 2024](#) found that MHW in the Chesapeake Bay follow two regimes: a spring-summer regime where temperature anomalies are confined to the mixed layer and a fall-winter regime that is more vertically homogeneous. The satellite observed seasonality in duration, with longest MHW in the winter, could be related to the presence of temperature anomalies throughout the water column and slower rates of decline due to the larger volume of water experiencing anomalies. Rates of onset and decline both have peaks in the Spring and Fall, although they differ in that rate of onset remains high in January/February while rate of decline decreases in this same period. The overall variation is large - with all characteristics experiencing at least a doubling between the minimum and maximum months.

The bay-wide average of about 25 MHW days per year is overall spatially uniform (Figure 11). Considering only MHW days, however, obscures significant spatial variability in the duration and frequency of MHWs in the Bay. Average number of annual

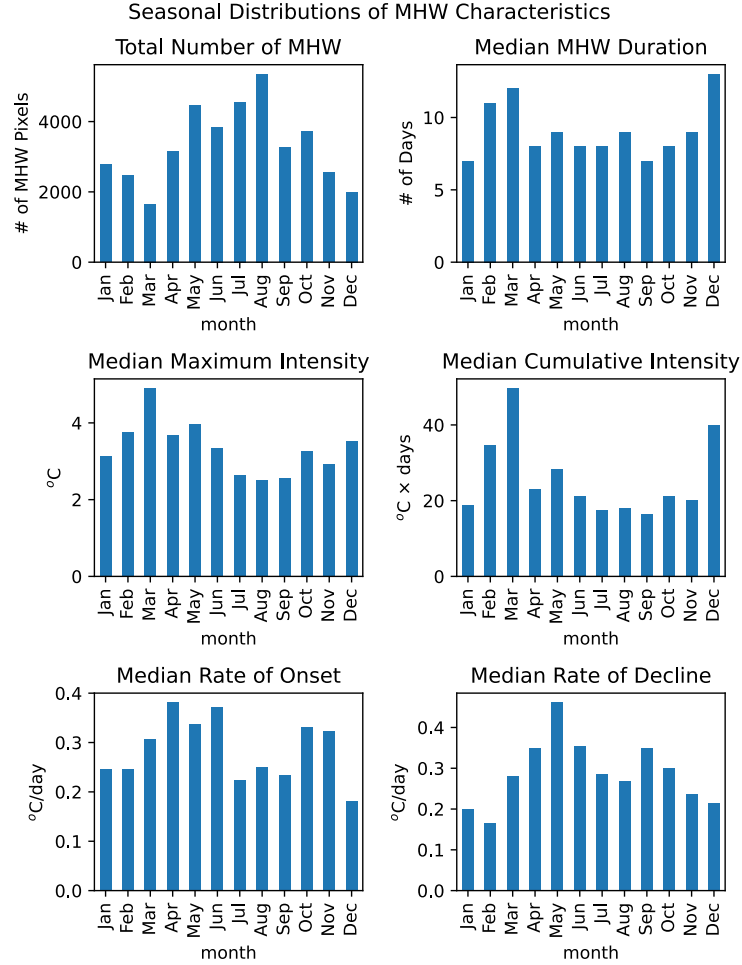


**Fig. 10** Monthly distributions of six MHW characteristics defined as shown in Figure 1. Each MHW is counted in the month in which it started. There is clear seasonality all of the characteristics, with an approximate doubling between maximum and minimum monthly values.

MHW and MHW duration show a north-south gradient, ranging from about 2-3 MHW per year and MHW durations between 8 and 13 days. The average number of annual MHW is highest in the northern areas of the Bay while the average MHW duration is highest in the southernmost regions of the Bay. The counteracting north-south gradients of these two fields leads to the uniform pattern of MHW days. To summarize, over the last 20 years in the Chesapeake Bay longer, less frequent heatwaves are found in the southern regions of the Bay while shorter, more frequent MHW characterize the northern regions. Spatial patterns such as this one are not evident when viewing averaged quantities, as the overall number of MHWs days does not vary significantly across the bay. In the following section we direct our focus to further consideration of spatial variability in MHW characteristics.

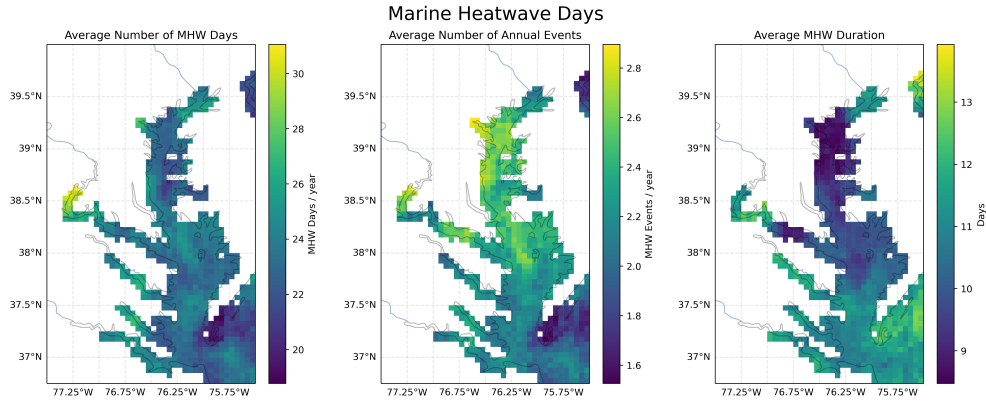


**Fig. 11** The spatial distribution of the average number of MHW days per year using Geo-Polar SST. The average number of MHW days is calculated by multiplying the average number per year by the average duration.

### 3.2 Marine Heatwave Characterization

Satellite observations give a finer grained look at the development and spatial structure of MHWs. This information can suggest physical mechanisms behind MHW development or decay or provide higher resolution insights for resource managers. Here we look at spatial variability in 6 MHW characteristics, each of which indicates something different about the evolution or potential impact of the MHW. The 6 characteristics are: 1) Average number of annual events 2) Average MHW duration 3) Average maximum intensity 4) Average cumulative intensity 5) Average rate of onset 6) Average rate of decline. The first two characteristics are shown in Figure 11 and the remaining 4 characteristics are shown in Figure 12.

MHW characteristics were aggregated to produce maps showing the average value for each characteristic across the full 20 year time series. The end result is 6 maps, one for each of the aggregated MHW characteristics across the Bay. In addition to the 6 aggregated characteristics in the diagram, average intensity was considered, but was found to closely follow the maximum intensity so it is not shown here.

The dominant pattern of spatial variation in MHW characteristics is a north-south gradient in the number of events and duration, as discussed in section 3.1. This north-south pattern was also evident in cumulative intensity. Cumulative intensity is a reflection of two aspects of a heatwave: duration and intensity. A MHW can have high cumulative intensity either because the MHW has a long duration, it has high maximum intensity, or both. In the Chesapeake Bay, MHW cumulative intensity is largest near the mouth of the Bay and minimum in the upper bay, suggesting it is more strongly influenced by duration than by maximum intensity (Figure 12). Average MHW duration doubles between the lowest and highest values in the Bay, while average maximum intensity changes by only a factor of about 1.3.

The exception to this north-south trend is areas of high river influence, including the upper bay where the Susquehanna River enters the Bay. These areas of river



## MHW Characteristic Maps

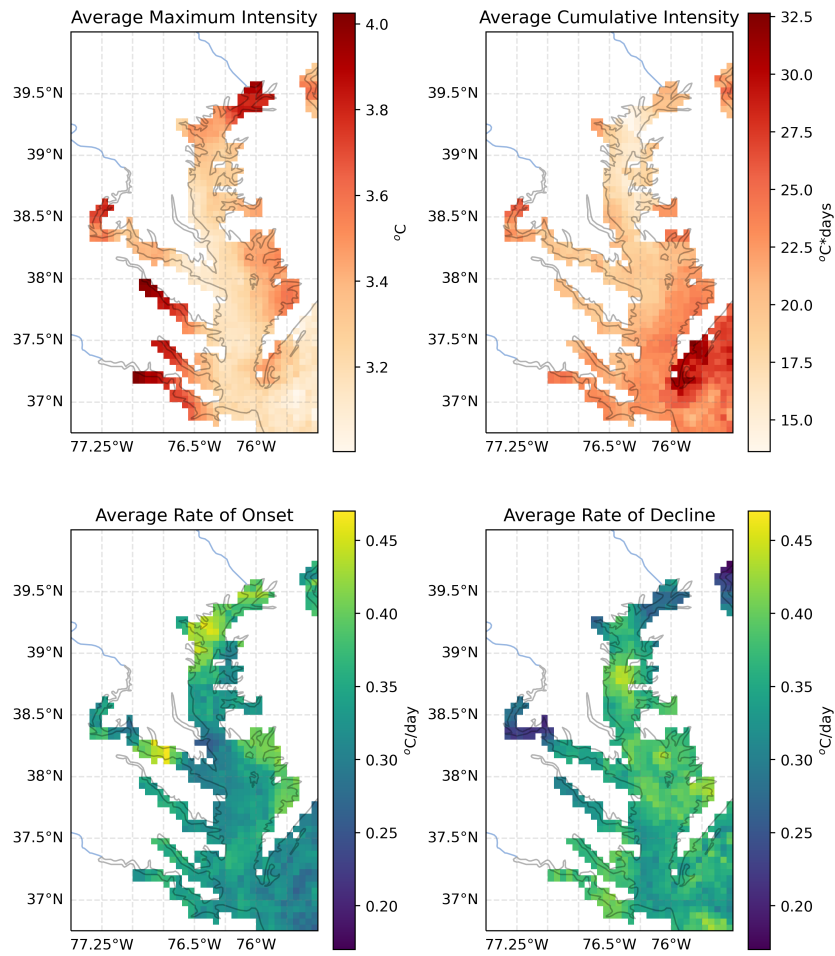


**Fig. 12** Spatial maps showing the distribution of 4 MHW characteristics. Maps show an aggregation (either sum or average) of across time for each pixel.

outflow show the largest maximum intensities and a consistent duration of about 12 days, irrespective of latitude (Figure 11, 12). While we cannot make strong conclusions about the Rappahannock, York, or James rivers, the two largest river inputs to the Bay, the Potomac river and Susquehanna outflow, are well sampled in our validation (see Section 2.4). Because maximum intensity is the maximum temperature anomaly relative to the climatological baseline and not the number of degrees above the 90th percentile threshold, high maximum intensities could be a result of larger standard deviation in temperature values in a particular section of the Bay. The high maximum intensity could also be related to depth, as the shallower water may heat

more effectively during a MHW, however we did not find depth to be strongly correlated to MHW intensity (not shown here). Past work has shown that low-land rivers are extremely sensitive to air temperature (Piccolroaz et al (2018)), a common driver of marine heatwaves.

Rate of onset and decline are two particularly important characteristics for understanding mechanisms of MHW development and decline. Rate of onset showed an approximately 1.5-fold difference between the highest and lowest values in the Bay, with some longitudinal variation (Figure 12). MHW develop the quickest in the upper Bay where temperature anomalies can increase at almost  $0.5^{\circ}\text{C}$  per day. Relative to rate of onset, rate of decline is more uniform in the main stem of the bay (approximately  $0.4^{\circ}\text{C}/\text{day}$ ). Shunk et al (2024) found that air-estuary heat flux changes, primarily from latent heat, is the leading driver of MHW onset and decline. However, the spatial variability in rates of onset and decline in the satellite data may suggest an additional role for other processes in the development and decay of MHW in the main stem of the Bay. Further investigation into the finer scale spatial structure of the rates of onset and decline could be an avenue of future research into drivers of MHW in the Bay.

### 3.3 Long Term Marine Heatwave Trends

To aid in understanding changes over time an analysis of long term trends in MHW characteristics is performed. To calculate the long term trend each pixel is treated as an independent time series. Each time series is grouped into annual bins and average MHW characteristics are computed per year. These annual values were then fit to a linear trend and the slope and significance were calculated for the 20 year times series. Significance testing was performed using a one-sided student t-test on each pixel in the bay and spatial patterns were evaluated using multiple hypothesis testing (Wilks, 2016). Multiple hypothesis testing accounts for the number of false positive trends that would be expected in a sample of our size using a false discovery rate, here set to 10%.

The data suggest that almost the entire Bay is experiencing significant increases in the number of annual MHW events (Figure 13). The largest values are just below an increase of 0.5 events / year, which is equivalent to about 5 additional MHW events per decade, or an approximately 10% increase in number of annual MHW events over the period of 2003-2022. There is significant spatial variation, seen in the factor of 3 increase between the slowest and fastest rates in the lower and upper Bay. The upper Bay, which experiences the most frequent but shortest MHW, is also the area that has the greatest increases in number of MHW. The only section of the Bay that does not see significant increases in number of events is the mouth of the Bay. In contrast, average duration and cumulative intensity did not show statistically significant increases over this time period. Given that cumulative intensity structure was controlled by duration we would expect that these two would show a similar trend, or lack thereof. In summary, we are seeing that for most of the main stem of the Bay, the qualitative character of MHWs are not changing, as MHWs are not longer nor are they more intense, but there are more MHWs occurring. This extends the findings of Mazzini and Pianca (2022), who found increases in frequency but no trend in duration at several moorings in the Bay over their study period, 1986-2020.

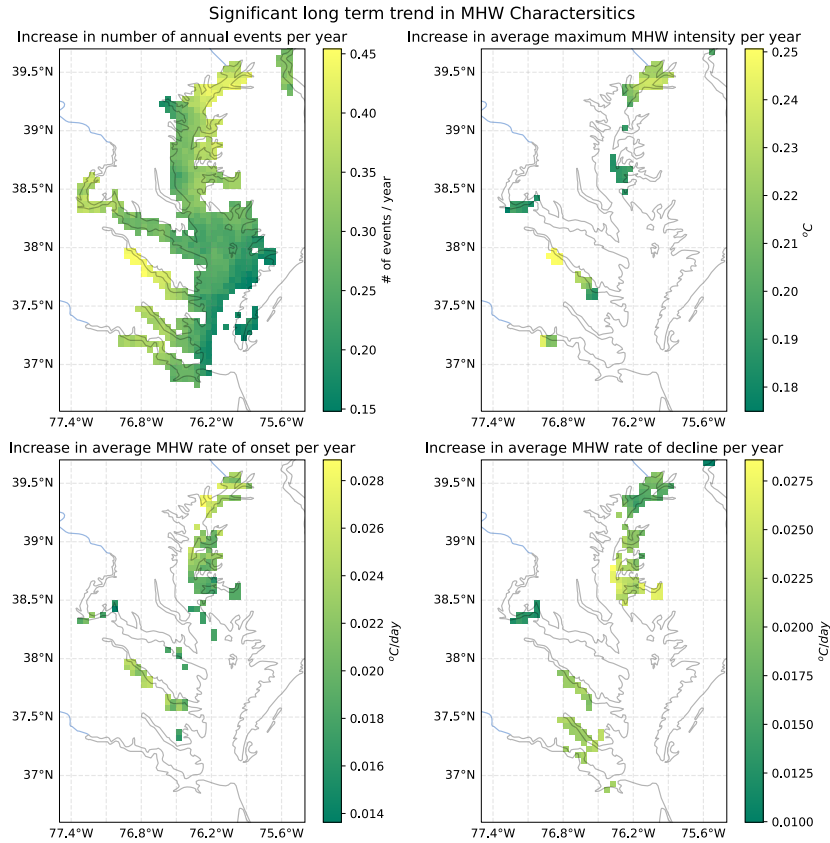


**Fig. 13** Long term trends in MHW characteristics. Plots show the slope of a linear regression on each pixel. Only those pixels considered statistically significant under multiple hypothesis testing with a false discovery rate of 10% were included.

The error analysis in section 2.4 revealed a spatial trend in the long term error with spatial variation in the error of the long term trend having a pattern that mirrors the observed trend in number of MHW: largest in the upper Bay and decreasing to the south. However, the observed long term increase in anomaly error, maximum of about  $1.5^{\circ}\text{C}/\text{decade}$ , is still less than the observed long term trend in MHW intensity, maximum of about  $2.5^{\circ}\text{C}/\text{decade}$  (Figure 7), giving some confidence in the result.

The exception to the north-south gradient in MHW trends is again the tributaries. The upper Potomac River, Rappahannock River and Susequhanna outflow show some areas with significant increases in maximum MHW intensity and rates of onset and decline. The main stem of the Bay does not show a significant trend in any characteristic except number of annual events. This is consistent with past work showing significant increases in US river temperatures, including the Potomac River (Kaushal et al, 2010).

While a large body of MHW literature has centered on the definition of a MHW with a steady climatological baseline described in Hobday et al (2016), there is a growing

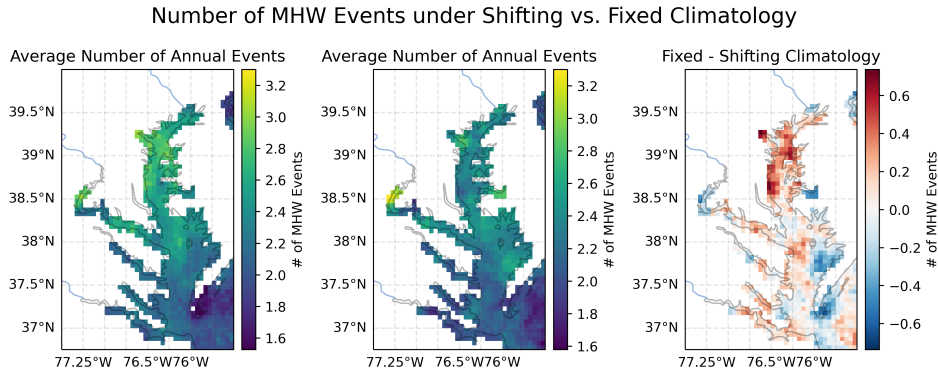


**Fig. 14** Comparison of MHW computed from a steady baseline with MHW computed using a detrended SST for the climatological baseline for the number of annual MHW events. All plots show steady baseline characteristic minus the detrended baseline characteristic. Red zones show where MHW characteristics are attributable to long term warming. We see strong influence of long term warming on MHW intensity in the upper rivers, in rate of onset in the upper bay, and in decreasing the north/south gradient of annual events and duration.

body of work utilizing a detrended SST for the climatological baseline (ex. (Jacox et al, 2020)). These two approaches provide different insights into future change and resource management (Amaya et al, 2023). Here we calculate annual number of MHW events with a detrended SST to highlight which aspects of the spatial pattern are related to long term warming as opposed to changes in extreme events (Figure 14). The north/south gradient in average duration and number of MHW per year is not present in the detrended MHW analysis. This suggests that the processes that generate the north/south gradient of longer MHW in the lower Bay are influenced by long term warming, consistent with the stronger lower Bay surface warming observed in Hinson et al (2022).

These data suggest that changes in MHW are not due to changes in spread of temperatures, or an increase in extreme values, but rather due to changes in the mean temperature. There are no significant long term trends in any MHW characteristic when computing MHW using the detrended climatology, evidence of the prior point. Past work has also attributed MHW trends to a long term change instead of increases in extreme temperature values Mazzini and Pianca (2022).

Past work has also investigated long term warming in the Chesapeake Bay. Hinson et al (2022) show that the strongest rates of surface warming occur at the mouth of the Bay, while the weakest warming is in the middle of the Bay. The authors specifically assess the oceanic influence on long term warming and find it to be the largest influence on long term warming in polyhaline waters (near the mouth of the Bay) June through September, the same time as when number of MHW peaks. In this main stem of the Bay this is the opposite of the trend observed in our data, where the lower Bay shows the weakest increase in number of MHW and no increase in MHW intensity. This may be because of the relatively small changes in average temperature: Hinson et al (2022) find a maximum 30 year temperature increase of about  $0.8^{\circ}\text{C}$ , or only  $0.027^{\circ}\text{C}/\text{year}$ . This is lower than the lowest significant increases in MHW intensity from our analysis.

Alternately, the differences in the long term vs. MHW analysis may suggest that the baseline shifts push temperature anomalies just over the MHW threshold. Where our results and [Hinson et al \(2022\)](#) agree is that temperatures are increasing more rapidly in the tributaries than in the main stem of the Bay.

## 4 Discussion

Estuarine environments provide critical ecological and economic value, however studies of estuarine marine heatwaves have been scarce. Availability of monitoring data is a common limitation, and buoy data does not provide highly resolved spatial structure. Here we used satellite data to provide a novel, spatially resolved picture of MHW in the Chesapeake Bay.

Two satellite SST sources, NASA MUR and NOAA Geo-Polar, were evaluated against in situ measurements. Both datasets likely underestimate extreme values and over estimate summertime long term trends, but show spatial consistency in SST anomalies. Validation work such as this is critical for accurate interpretation of global SST datasets in coastal zones. This validation was possible because of the availability of in situ validation data, but this resource is not available in every estuary. Successful use of satellite SST in the Chesapeake supports the possibility that satellite SST may be used for studying temperature in other large estuaries where a lack of in situ data may render independent validation experiments unfeasible.

MHW characteristic maps reveal significant spatial variation in the Chesapeake, where the dominant pattern of variability is a north to south (along estuary) gradient. Spatial structure reveals that cumulative intensity is dominated by MHW duration, not max intensity. This result, coupled with the strong bay wide variation in MHW duration, highlight MHW duration as a key MHW characteristic in the Chesapeake Bay. Temporal MHW analyses show increases in MHW frequency over time and an average of 25 MHW days per year bay-wide. Increases in MHW events in the lower bay result in approximately 5 additional annual events per decade, a near doubling of MHW frequency over the 20 year satellite period. Comparison of these results with a detrended SST analysis suggest that long term warming influence on MHW characteristics is particularly influential in zones of river influence. Satellite-derived MHW analysis is consistent with past buoy based analysis, giving confidence in the accuracy of this new technique. Given that the satellite data likely represents and underestimate of temperature (Section 2.4), it is possible these trends are even stronger. Increased spatial resolution and clarity into regional trends in MHW characteristics benefits our understanding of extreme temperature events in the Chesapeake Bay and could benefit monitoring efforts that help mitigate the high economic impact and conserve protected waters.

Future analysis could focus on connecting spatial patterns of MHW characteristics identified here to MHW mechanisms of development and decline in the Chesapeake. Patterns of evolution, such as the example in Figure 8, hint at multiple spatial patterns of evolution that could indicate differing influences. For example, some MHW appeared to develop starting in the river tributaries and expand to the main stem,

while others appeared to begin at the mouth of the Bay, perhaps reflecting the relative influence of rivers and the coastal ocean. Another avenue could be to pursue the spatial patterns in rates of onset and decline. Past work in the North Atlantic suggests atmospheric mechanisms to be the most influential mechanism in MHW development while ocean processes to be the more influential mechanism in MHW decline (Schlegel et al, 2021). Rate of onset and decline in the Chesapeake Bay showed the finest scale spatial structure of the metrics considered here, and differences in their distributions could be related to mechanistic influence.

The Chesapeake Bay is the largest estuary in the US and the impacts of a warming climate have societal and economic impact. This work provides a spatial analysis of MHW characteristics and trends in the Chesapeake. Validation of satellite SST in the Bay allows future researchers to more accurately understand results derived using SST in the Bay. Spatial variation in MHW characteristics highlights the importance of spatial structure in the Bay, highlights the differences between river regions and main stem waters, and provides initial insight into possible MHW mechanisms.

## 5 Declarations

### 5.1 Funding

This study was supported by NOAA grant NA19NES4320002 (Cooperative Institute for Satellite Earth System Studies-CISESS) at the University of Maryland/ESSIC. Jacob Wenegrat acknowledges support from NSF award 2126474. The scientific results and conclusions, as well as any views or opinions expressed herein, are those of the author(s) and do not necessarily reflect the views of NOAA or the Department of Commerce.

### 5.2 Competing Interests

The authors certify that they have no affiliations with or involvement in any organization or entity with any financial interest or non-financial interest in the subject matter or materials discussed in this manuscript.

### 5.3 Code Availability

The code associated with the article can be accessed via Github: [https://github.com/rwegener2/article\\_chesapeake\\_marineheatwaves](https://github.com/rwegener2/article_chesapeake_marineheatwaves)

### 5.4 Author Contribution

Rachel Wegener: Conceptualization, Methodology, Software, Investigation, Data curation, Writing - Original Draft, Visualization. Jacob Wenegrat: Conceptualization, Methodology, Writing - Review & Editing, Supervision, Project administration. Veronica P. Lance: Conceptualization, Methodology, Writing - Review & Editing, Supervision, Funding acquisition. Skylar Lama: Software, Formal analysis, Data curation.

## References

- Amaya DJ, Jacox MG, Fewings MR, et al (2023) Marine heatwaves need clear definitions so coastal communities can adapt. *Nature* 616(7955):29–32. <https://doi.org/10.1038/d41586-023-00924-2>, URL <https://www.nature.com/articles/d41586-023-00924-2>, bandiera\_abtest: a Cg.type: Comment Publisher: Nature Publishing Group Subject.term: Ocean sciences, Policy, Climate change, Society
- Batiuk R, Brownson K, Dennison W, et al (2023) Rising watershed and bay water temperatures: Ecological implications and management responses – a stac workshop
- Beggs H (2020) Chapter 14: Temperature, in: *Earth observation: Data, processing and applications. volume 3b: Applications – surface waters* (eds. harrison, b.a., anstee, j.a., dekker, a., phinn, s., mueller, n., byrne, g.) crcsi, melbourne.
- Bilkovic DM, Mitchell MM, Havens KJ, et al (2019) Chapter 15 - chesapeake bay. In: Sheppard C (ed) *World Seas: an Environmental Evaluation* (Second Edition). Academic Press, p 379–404, <https://doi.org/10.1016/B978-0-12-805068-2.00019-X>, URL <https://www.sciencedirect.com/science/article/pii/B978012805068200019X>
- Chin TM, Vazquez-Cuervo J, Armstrong EM (2017) A multi-scale high-resolution analysis of global sea surface temperature. *Remote Sensing of Environment* 200:154–169. <https://doi.org/10.1016/j.rse.2017.07.029>, URL <https://www.sciencedirect.com/science/article/pii/S0034425717303462>
- Du J, Shen J, Park K, et al (2018) Worsened physical condition due to climate change contributes to the increasing hypoxia in chesapeake bay. *Science of The Total Environment* 630:707–717. <https://doi.org/10.1016/j.scitotenv.2018.02.265>, URL <https://linkinghub.elsevier.com/retrieve/pii/S004896971830665X>
- Gawarkiewicz G, Chen K, Forsyth J, et al (2019) Characteristics of an advective marine heatwave in the middle atlantic bight in early 2017. *Frontiers in Marine Science* 6. URL <https://www.frontiersin.org/articles/10.3389/fmars.2019.00712>
- Hinson KE, Friedrichs MA, St-Laurent P, et al (2022) Extent and causes of chesapeake bay warming. *J American Water Resour Assoc* 58(6):805–825. <https://doi.org/10.1111/1752-1688.12916>, URL <https://onlinelibrary.wiley.com/doi/10.1111/1752-1688.12916>
- Hobday AJ, Alexander LV, Perkins SE, et al (2016) A hierarchical approach to defining marine heatwaves. *Progress in Oceanography* 141:227–238. <https://doi.org/10.1016/j.pocean.2015.12.014>, URL <https://www.sciencedirect.com/science/article/pii/S0079661116000057>
- Jacox MG, Alexander MA, Bograd SJ, et al (2020) Thermal displacement by marine heatwaves. *Nature* 584(7819):82–86. <https://doi.org/10.1038/s41586-020-2534-z>,

- URL <https://www.nature.com/articles/s41586-020-2534-z>, publisher: Nature Publishing Group
- Kaushal SS, Likens GE, Jaworski NA, et al (2010) Rising stream and river temperatures in the United States. *Frontiers in Ecology and the Environment* 8(9):461–466. <https://doi.org/10.1890/090037>, URL <https://onlinelibrary.wiley.com/doi/abs/10.1890/090037>, eprint: <https://esajournals.onlinelibrary.wiley.com/doi/pdf/10.1890/090037>
- Lefcheck JS, Wilcox DJ, Murphy RR, et al (2017) Multiple stressors threaten the imperiled coastal foundation species eelgrass (*zostera marina*) in chesapeake bay, USA. *Global Change Biology* 23(9):3474–3483. <https://doi.org/10.1111/gcb.13623>, URL <https://onlinelibrary.wiley.com/doi/abs/10.1111/gcb.13623>, eprint: <https://onlinelibrary.wiley.com/doi/pdf/10.1111/gcb.13623>
- Maturi E, Harris A, Mittaz J, et al (2017) A new high-resolution sea surface temperature blended analysis. *Bulletin of the American Meteorological Society* 98(5):1015–1026. <https://doi.org/10.1175/BAMS-D-15-00002.1>, URL <https://journals.ametsoc.org/view/journals/bams/98/5/bams-d-15-00002.1.xml>, publisher: American Meteorological Society Section: Bulletin of the American Meteorological Society
- Mazzini P, Pianca C (2022) Marine heatwaves in the chesapeake bay. *Frontiers in Marine Science* 8. URL <https://www.frontiersin.org/articles/10.3389/fmars.2021.750265>
- Mills KE, Pershing AJ, Brown CJ, et al (2013) Fisheries management in a changing climate: Lessons from the 2012 ocean heat wave in the northwest atlantic. *Oceanography* 26(2):191–195. URL <https://www.jstor.org/stable/24862052>, publisher: Oceanography Society
- Oliver E (2023) marineheatwaves. <https://github.com/ecjoliver/marineHeatWaves>
- Oliver ECJ, Donat MG, Burrows MT, et al (2018) Longer and more frequent marine heatwaves over the past century. *Nature Communications* 9(1):1324. <https://doi.org/10.1038/s41467-018-03732-9>, URL <https://doi.org/10.1038/s41467-018-03732-9>
- Oliver ECJ, Burrows MT, Donat MG, et al (2019) Projected marine heatwaves in the 21st century and the potential for ecological impact. *Frontiers in Marine Science* 6. URL <https://www.frontiersin.org/articles/10.3389/fmars.2019.00734>
- Pershing AJ, Mills KE, Dayton AM, et al (2018) Evidence for adaptation from the 2016 marine heatwave in the northwest atlantic ocean. *Oceanography* 31(2):152–161. URL <https://www.jstor.org/stable/26542661>, publisher: Oceanography Society



- Piccolroaz S, Toffolon M, Robinson CT, et al (2018) Exploring and Quantifying River Thermal Response to Heatwaves. *Water* 10(8):1098. <https://doi.org/10.3390/w10081098>, URL <https://www.mdpi.com/2073-4441/10/8/1098>, number: 8 Publisher: Multidisciplinary Digital Publishing Institute
- Rahmstorf S, Coumou D (2011) Increase of extreme events in a warming world. *Proc Natl Acad Sci USA* 108(44):17905–17909. <https://doi.org/10.1073/pnas.1101766108>, URL <https://pnas.org/doi/full/10.1073/pnas.1101766108>
- Schlegel RW, Oliver ECJ, Hobday AJ, et al (2019) Detecting marine heatwaves with sub-optimal data. *Front Mar Sci* 6:737. <https://doi.org/10.3389/fmars.2019.00737>, URL <https://www.frontiersin.org/article/10.3389/fmars.2019.00737/full>
- Schlegel RW, Oliver ECJ, Chen K (2021) Drivers of marine heatwaves in the northwest atlantic: The role of air–sea interaction during onset and decline. *Frontiers in Marine Science* 8. URL <https://www.frontiersin.org/articles/10.3389/fmars.2021.627970>
- Shunk NP, Mazzini PLF, Walter RK (2024) Impacts of marine heatwaves on subsurface temperatures and dissolved oxygen in the chesapeake bay. *Journal of Geophysical Research: Oceans* 129(3):e2023JC020338. <https://doi.org/https://doi.org/10.1029/2023JC020338>, URL <https://agupubs.onlinelibrary.wiley.com/doi/abs/10.1029/2023JC020338>, e2023JC020338 2023JC020338, <https://agupubs.onlinelibrary.wiley.com/doi/pdf/10.1029/2023JC020338>
- Smith KE, Burrows MT, Hobday AJ, et al (2021) Socioeconomic impacts of marine heatwaves: Global issues and opportunities. *Science* 374(6566):eabj3593. <https://doi.org/10.1126/science.abj3593>, URL <https://www.science.org/doi/10.1126/science.abj3593>
- Smith KE, Burrows MT, Hobday AJ, et al (2023) Biological impacts of marine heatwaves. *Annual Review of Marine Science* 15(1):119–145. <https://doi.org/10.1146/annurev-marine-032122-121437>, URL <https://doi.org/10.1146/annurev-marine-032122-121437>, eprint: <https://doi.org/10.1146/annurev-marine-032122-121437>
- Wilks DS (2016) “The Stippling Shows Statistically Significant Grid Points”: How Research Results are Routinely Overstated and Overinterpreted, and What to Do about It. *Bulletin of the American Meteorological Society* 97(12):2263–2273. <https://doi.org/10.1175/BAMS-D-15-00267.1>, URL <https://journals.ametsoc.org/view/journals/bams/97/12/bams-d-15-00267.1.xml>, publisher: American Meteorological Society Section: Bulletin of the American Meteorological Society